

Simulation of beam-beam effects and Tevatron experience

Alexander Valishev^{a*}, Yuri Alexahin^a, Valeri Lebedev^a and Dmitry Shatilov^b

^a*Fermi National Accelerator Laboratory,
PO Box 500, Batavia, IL, 60510 USA*

^b*Budker Institute of Nuclear Physics,
Novosibirsk, 630090, Russia*

E-mail: valishev@fnal.gov

ABSTRACT: Effects of electromagnetic interactions of colliding bunches in the Tevatron had a variety of manifestations in beam dynamics presenting vast opportunities for development of simulation models and tools. In this paper the computer code for simulation of weak-strong beam-beam effects in hadron colliders is described. We report the collider operational experience relevant to beam-beam interactions, explain major effects limiting the collider performance and compare results of observations and measurements with simulations.

KEYWORDS: Accelerator modelling and simulations; Beam dynamics.

*Corresponding author.

Contents

1. Introduction	1
2. Overview of beam-beam effects	2
2.1 Beam-beam effects at injection energy	3
2.2 Beam-beam effects during low-beta squeeze	4
2.3 Beam-beam effects during high energy physics operation	5
3. Multi-process beam physics analysis	7
4. Numerical simulations of beam-beam effects	8
4.1 Tevatron optics	10
4.2 Chromaticity	10
4.3 Diffusion and noise	11
4.4 Program features	13
4.5 Code validation	14
5. Simulation results	14
5.1 Optics errors	15
5.2 New collision helical separated orbit	16
5.3 Betatron tune chromaticity	17
5.4 β^* reduction	18
5.5 Second order chromaticity	18
6. Summary and discussion	20

1. Introduction

Peak luminosity of the Tevatron reached $4.3 \times 10^{32} \text{ cm}^{-2} \text{ s}^{-1}$, which exceeds the original Collider Run II goal [1]. This achievement became possible due to numerous upgrades in the antiproton source, injector chain, and in the Tevatron collider itself. One of the most notable rises of luminosity came from the commissioning of electron cooling in the Recycler Ring and advances in the antiproton accumulation rate [2]. Starting from 2007, the intensity and brightness of antiprotons delivered to the collider greatly enhanced the importance of beam-beam effects. Several configurational and operational improvements in the Tevatron have been planned and implemented in order to alleviate these effects and allow stable running at high peak luminosities.

Since the publication of paper [3] that gave a detailed summary of beam dynamics issues related to beam-beam effects, the peak luminosity of Tevatron experienced almost a three-fold increase. In the present article we provide an updated view based on the last years of collider operation (Section 2).

Development of a comprehensive computer simulation of beam-beam effects in the Tevatron started in 1999. This simulation proved to be a useful tool for understanding existing limitations and finding ways to mitigate them. As the first step, we developed a simplified model of beam parameter evolution in the Tevatron, which includes all important phenomena affecting luminosity decay, excluding the beam-beam effects (Section 3). For the numerical simulations of beam-beam effects, we used a multiparticle tracking code Lifetrac. In Section 4 the main features of the code are described. In Sections 5.2-5.5 we summarize our experience with simulations of beam-beam effects in the Tevatron, and cross-check the simulation results against various experimental data and analytical models. We also correlate the most notable changes in the machine performance to changes of configuration and beam conditions, and support the explanations with simulations.

2. Overview of beam-beam effects

A detailed description of the Tevatron collider Run II can be found elsewhere [1]. Here we provide only essential features important for understanding of the beam dynamics.

The Tevatron was a superconducting proton-antiproton collider ring in which beams of the two species collided at the center of mass energy of 2×0.98 TeV at two experiments. Each beam consisted of 36 bunches grouped in 3 trains of 12 with 396 ns bunch spacing and $2.6 \mu\text{s}$ abort gaps between the trains. The beams shared a common vacuum chamber with both beams moving along helical trajectories formed by electrostatic separators. Before the high energy physics collisions have been initiated, the proton and antiproton beams could be moved longitudinally with respect to each other, which is referred to as cogging. This configuration allowed for 72 interactions per bunch each turn with the total number of collision points in the ring equal to 138. The total number of collision points was determined by the symmetry of bunch filling pattern.

At the peak performance Tevatron operated with approximately $N_p = 2.8 \cdot 10^{11}$ protons and $N_a = 0.9 \cdot 10^{11}$ antiprotons per bunch at the beginning of a store. The normalized transverse 95% beam emittances were $\varepsilon_p = 18 \cdot 10^{-6} \text{m}$ for protons and $\varepsilon_a = 7 \cdot 10^{-6} \text{m}$ for antiprotons. The rms length of proton and antiproton bunches at the beginning of a high energy physics (HEP) store was 52 cm and 48 cm, respectively. Parameters of the beams were mostly determined by the upstream machines.

The value of β -function at the main collision points (β^*) was 0.28 m. Betatron tunes were $Q_x = 20.584$, $Q_y = 20.587$ for protons and $Q_x = 20.575$, $Q_y = 20.569$ for antiprotons.

A typical collider fill cycle is shown in Figure 1. First, proton bunches were injected one at a time on the central orbit. After that, the electrostatic separators were powered and antiproton bunches were injected in batches of four. This process was accompanied by longitudinal cogging after each 3 transfers. Then the beams were accelerated to the top energy in 85 s and the machine optics was changed to collision configuration in 25 steps over 120 seconds of the so-called low-beta squeeze, during which the β^* changed from 1.5 to 0.28 m. The last two stages included initiating collisions at the two main interaction points (IP) and removing halo by moving in the collimators.

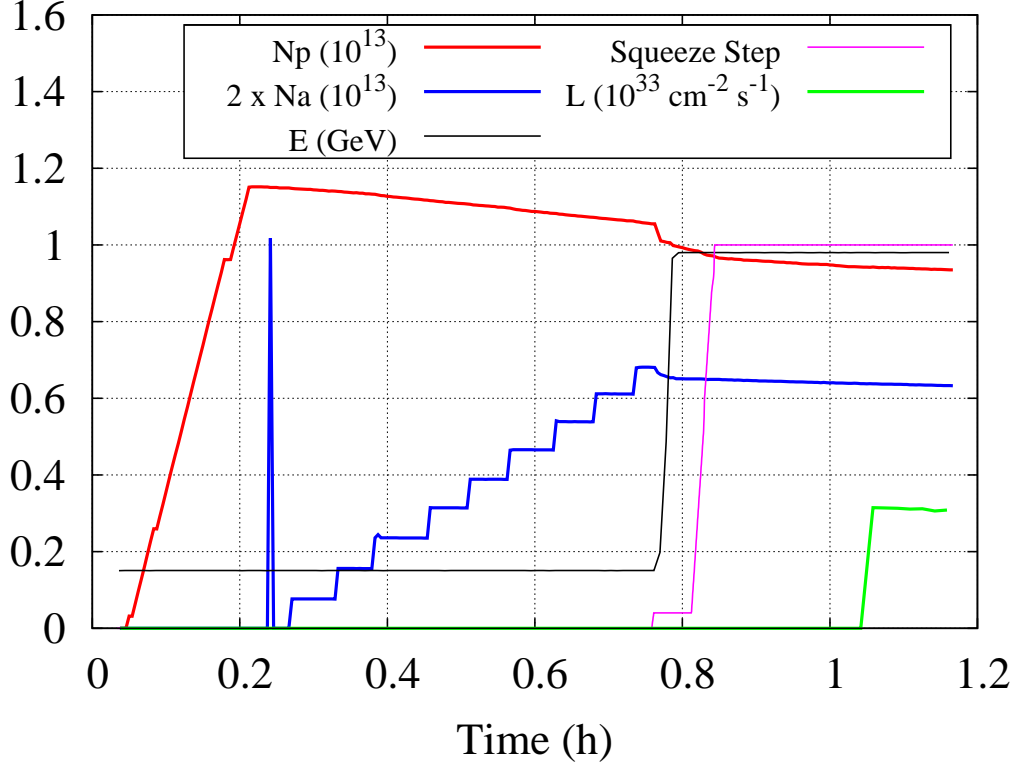


Figure 1. Collider fill cycle for store 5989.

It has been shown in machine studies that beam losses up the ramp and through the low-beta squeeze were mainly caused by beam-beam effects [3]. During the high energy physics collisions runs (HEP mode), the beam-beam induced emittance growth and particle losses contributed to the faster luminosity decay. Figure 2 summarizes the observed losses of luminosity during different stages of the collider cycle.

2.1 Beam-beam effects at injection energy

During injection the long range (also referred to as parasitic) beam-beam effects caused proton losses (usually 5 to 10%). At the same time the antiproton lifetime $(dN_a/dt/N_a)^{-1}$ was very good and only a fraction of a per cent were lost. Observations showed that mainly off momentum particles were lost (Figure 3) and the betatron tune chromaticity $C = dQ/d\delta$, where $\delta = \Delta p/p$ is the relative momentum deviation, had a remarkable effect. Early in Run II the chromaticity had to be kept higher than 8 units in order to maintain coherent stability of the intense proton beam, but after several improvements aimed at reduction of the machine impedance the chromaticity was about 3 units [4, 5, 6]. Figure 3 shows an interesting feature in the behavior of two adjacent proton bunches (no. 20 and 21). Spikes in the measured values are instrumental effects labeling the time when the beams are clogged. Before the first clogging the bunches have approximately equal lifetime. After the first clogging bunch 20 exhibits faster decay, and bunch 21 after the second. Analysis of the collision patterns for these bunches allowed to pinpoint a particular collision point responsible for

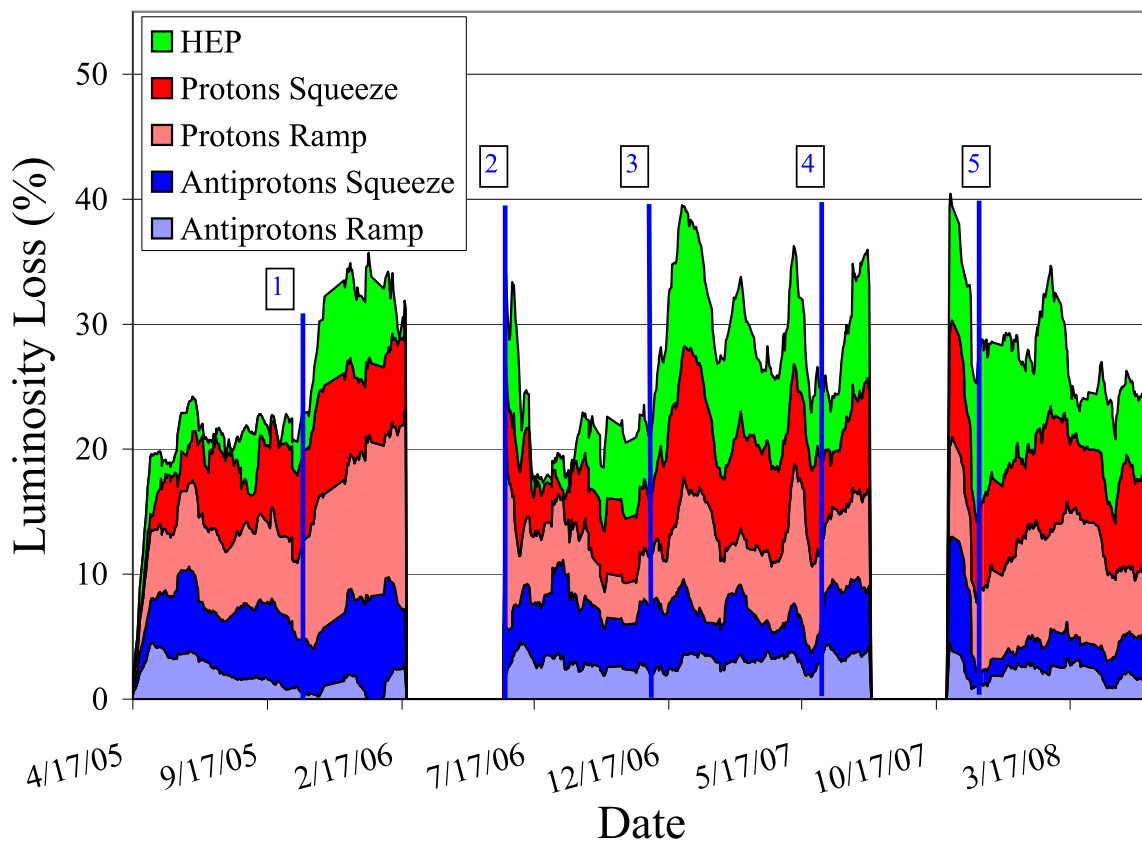


Figure 2. Luminosity loss budget over a 3 year period. The labels mark: 1. Commissioning of electron cooling. 2. Installation of extra separators and new collision helical orbit. 3. Improved antiproton accumulation rate (stochastic cooling upgrade). 4. Correction of second-order chromaticity. 5. Implementation of controlled antiproton emittance blowup.

the lifetime degradation. The new optimized helical orbit separation scheme at injection energy has been implemented late in 2007 which improved the proton lifetime [7, 8].

2.2 Beam-beam effects during low-beta squeeze

During the low-beta squeeze two significant changes occurred - the β^* value was being gradually decreased from ~ 1.5 m to 0.28 m (hence the name squeeze) and the helical orbits changed their shape and polarity from injection to collision configuration. The latter posed a serious limitation since the beams separation at several long range collision points briefly decreased from $5-6\sigma$ to $\sim 2\sigma$. At this moment a sharp spike in losses was observed.

Another important operational concern was the tight aperture limitation in one of the two final focus regions (CDF). With dynamically changing orbit and lattice parameters the local losses were often high enough to cause a quench of the superconducting magnets even though the total amount of beam loss was small ($\sim 1\%$). The aperture restriction has been located and fixed in October of 2008.

Besides orbit stability two other factors were found to be important in maintaining low losses through the squeeze: antiproton beam brightness and betatron coupling. Figure 4 shows the de-

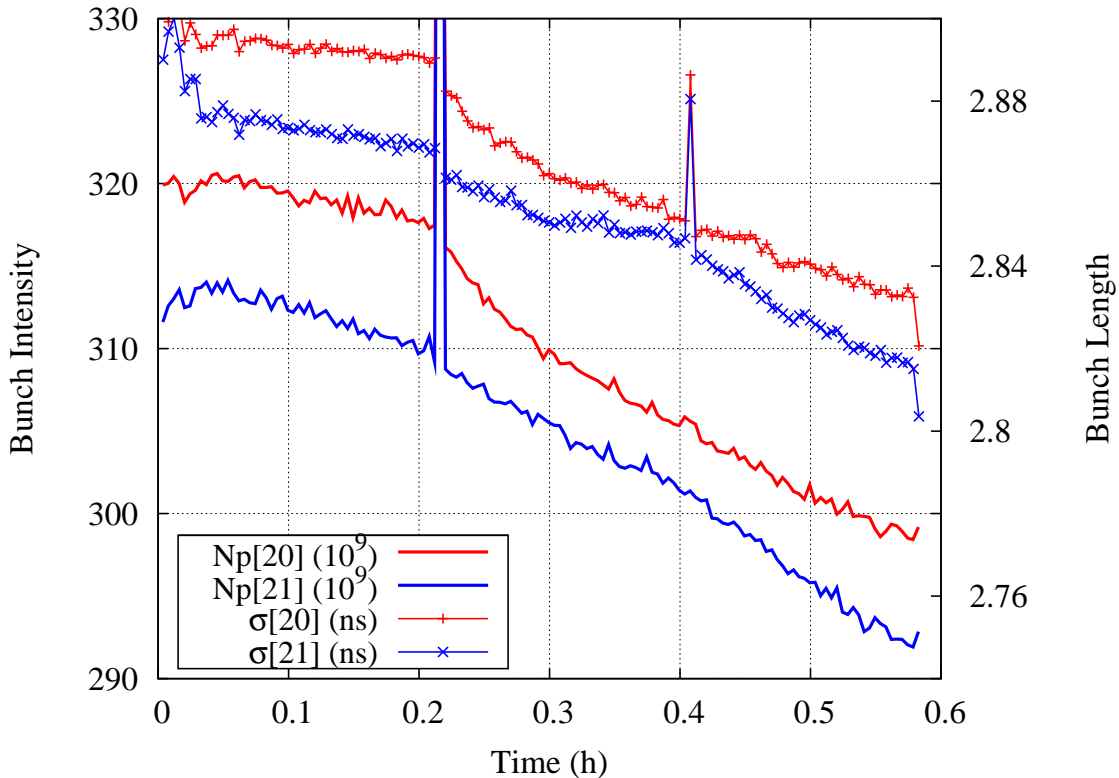


Figure 3. Intensity and rms length (ns) of proton bunches no. 20 and 21 during injection of antiprotons.

pendence of proton losses on the antiproton beam brightness. Improvements implemented in the antiproton source during the 2007 shutdown resulted in the increase of antiproton beam brightness. This, in turn, caused a large number of stores to be lost at that stage of the Tevatron cycle, and hence demanded the commissioning of antiproton emittance control system [9].

2.3 Beam-beam effects during high energy physics operation

After the beams were brought into collisions at the main IPs, there were two head-on and 70 long range collision points per bunch. Beam-beam effects caused by these interactions lead to emittance growth and particle losses in both beams.

During the running prior to the 2006 shutdown the beam-beam effects at HEP mostly affected antiprotons. The long range collision points nearest to the main IPs were determined to be the leading cause for poor lifetime. Additional electrostatic separators were installed in order to increase the separation at these IPs from 5.4 to 6σ [8]. Also, the betatron tune chromaticity was decreased from 20 to 10 units. Since then, the antiproton lifetime was dominated by losses due to luminosity and no emittance growth was observed provided that the betatron tune working point was well controlled.

Commissioning of electron cooling of antiprotons in the Recycler resulted in smaller emittances, which together with increased antiproton stacking rate drastically changed the situation for protons. Figure 5 shows the evolution of total head-on beam-beam tune shift $\xi = Nr_p/4\pi\epsilon$ (where

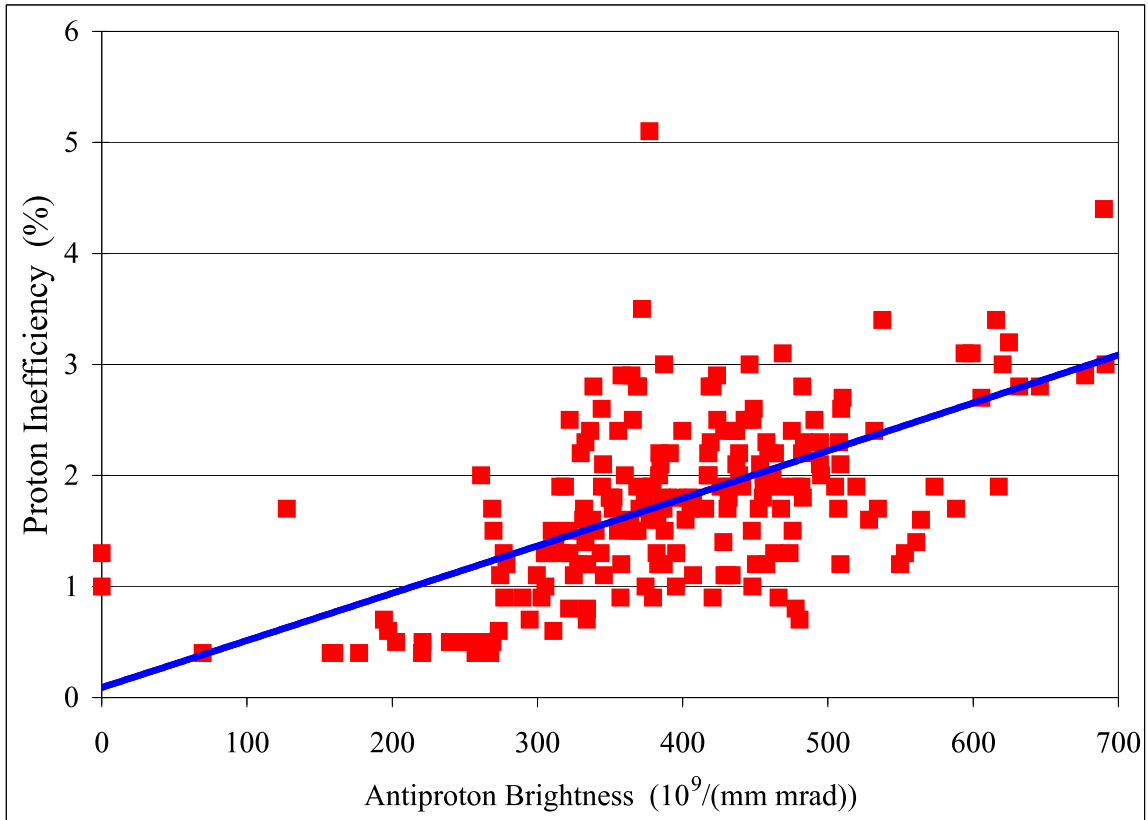


Figure 4. Proton losses during low-beta squeeze vs. antiproton beam brightness $36 \cdot N_a / \epsilon_a$.

N is the number of particles, r_p is the classical proton radius, ϵ is the normalized rms emittance) for protons and antiprotons. Note that prior to the 2006 shutdown the proton ξ was well under 0.01 and big boost occurred in 2007 when both beam-beam parameters became essentially equal. It was then when beam-beam related losses and emittance blowup started to be observed in protons.

Our analysis showed that deterioration of the proton lifetime was caused by a decrease of the dynamical aperture for off-momentum particles due to head-on collisions (see Sec. 5.5). It was discovered that the Tevatron optics had large chromatic perturbations, e.g. the value of β^* for off-momentum particles could differ from that of the reference particle by as much as 20%. Also, the high value of second order betatron tune chromaticity $d^2Q/d(\Delta p/p)^2$ generated a tune spread of ~ 0.002 . A rearrangement of sextupoles in order to correct the second order chromaticity has been planned and implemented in 2007 shutdown [10]. Figure 6 demonstrates the effect of this modification on the integrated luminosity. The time dependence of luminosity is very well approximated by $L_0/(1+t/\tau)$. Therefore one can normalize the luminosity integral for a given store to a fixed length T_0 by using the expression $L_0\tau \cdot \ln(1+T_0/\tau)$ [11]. Here L_0 is the initial luminosity, and τ is the luminosity lifetime. One can see that after the modification the saturation at luminosities above $2.6 \times 10^{32} \text{cm}^{-2}\text{s}^{-1}$ was mitigated and the average luminosity delivered to experiments increased by some 10%.

Another increase in the proton ξ occurred after the 2007 shutdown when the transverse antiproton emittance was decreased due to improvements in the injection optics matching. The total

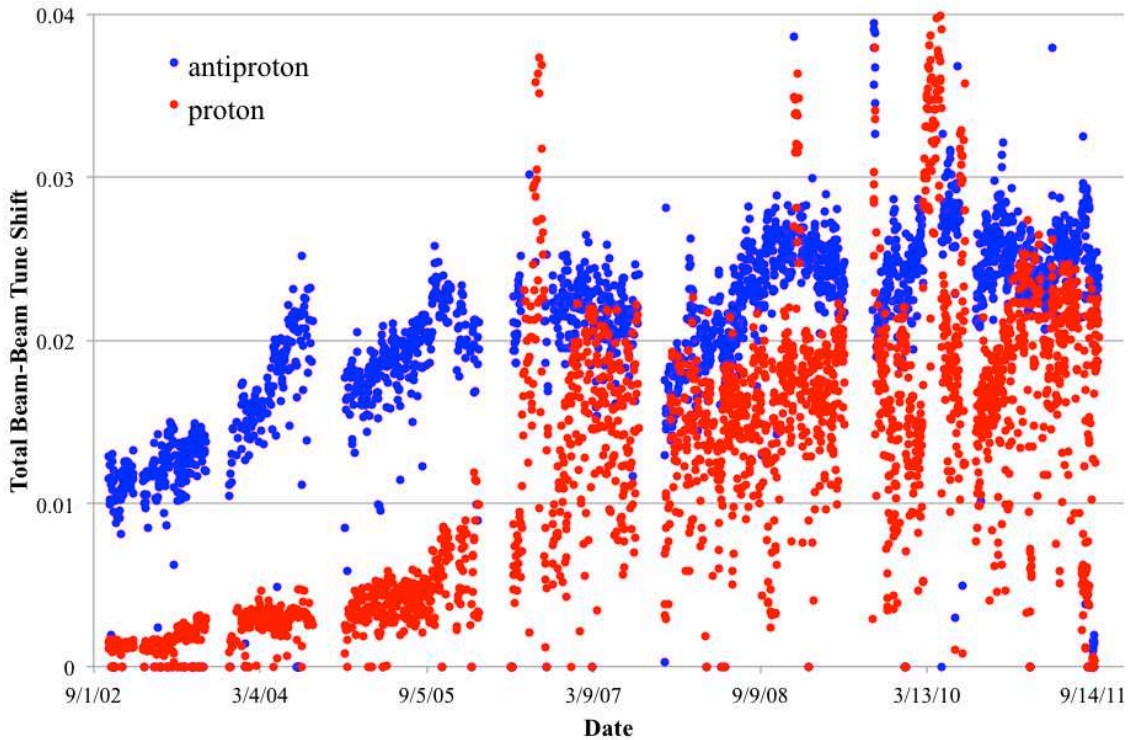


Figure 5. Head-on beam-beam tune shift parameter vs. time.

attained head-on beam-beam tune shift for protons became higher than that of antiprotons and exceeded 0.03. That led to high sensitivity of the proton lifetime to minor variations of the betatron tunes, and to severe background conditions for the experiments. The reason was believed to be the large betatron tune spread generated by significantly unequal beam sizes at the IPs [12]. Indeed, at times the antiproton beam size was a factor of 2 to 2.5 smaller than the proton size.

A dedicated system has been commissioned to reduce the proton-to-antiproton emittance ratio. It increased the antiproton emittance after the top energy was reached by applying wide band transverse noise to a directional strip line (line 5 in Fig. 2) [9]. Ultimately, the optimal emittance ratio for operations was determined to be about 3 (i.e. the factor of 1.7 in beam sizes).

The remaining part of this paper deals with beam-beam effects in the HEP stores. Discussions on the long range effects at the injection energy and coherent beam-beam effects [13] are left out of the scope of this report.

3. Multi-process beam physics analysis

The beam-beam interaction was not the single strongest effect determining the evolution of beam parameters at collisions. There were other sources of diffusion causing the emittance growth and particle losses, including the intrabeam scattering, noise of accelerating RF voltage, ground motion, scattering on the residual gas, and particle burnup due to luminosity (non-elastic scattering). Parameters of these mechanisms were measured in beam studies (see e.g. [26]), and then a model was built in which the equations of diffusion and other processes were solved numerically [14].

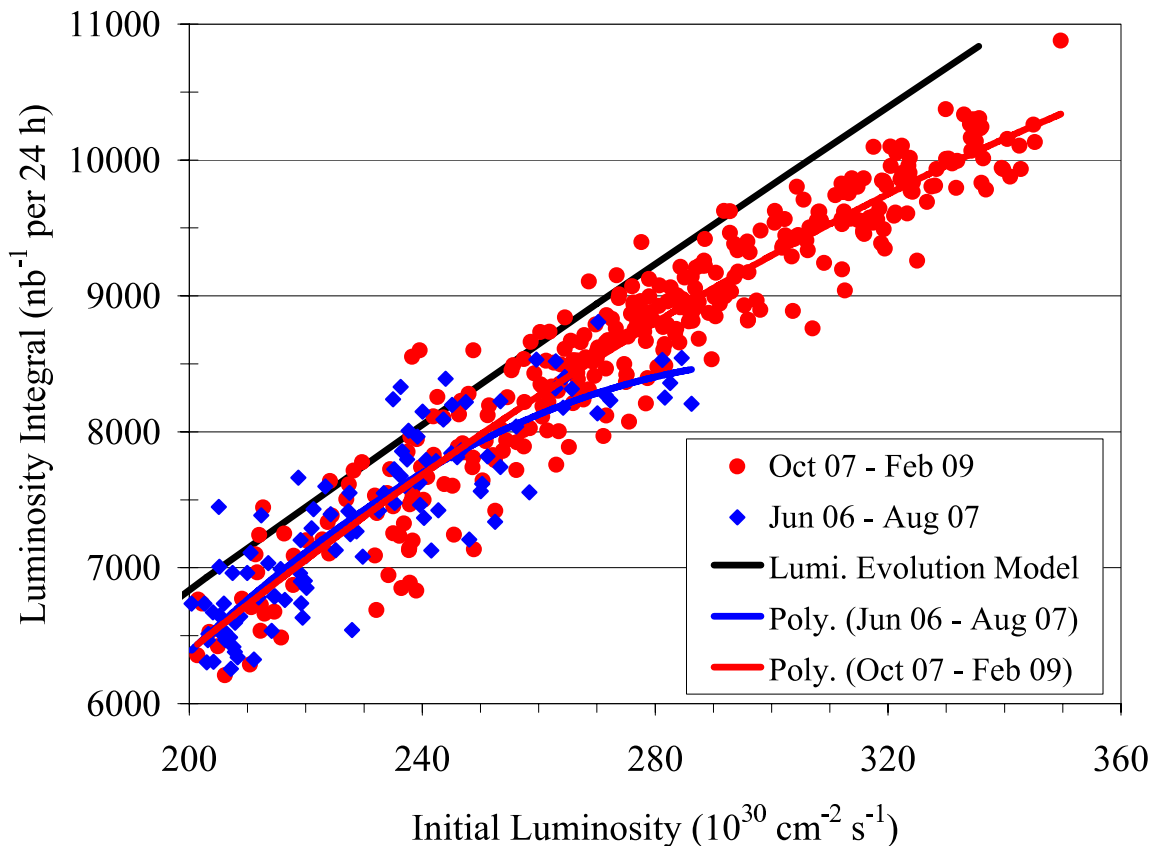


Figure 6. Luminosity integral normalized for 24 hrs store vs. initial luminosity. Blue points and curve - before the second order chromaticity correction, red - after the correction. Black line represents the maximum possible luminosity integral for the given beam parameters in the absence of beam-beam effects.

This model was able to predict evolution of the beam parameters in the case of weak beam-beam effects. When these effects are not small, it provides a reference for evaluation of their strength. We used that analysis on a store-by-store basis to monitor the machine performance in real time [15] because such calculations were very fast compared to a full numerical beam-beam simulation. Figure 7 presents an example comparison of the evolution of beam parameters in an actual high luminosity store to the calculations. Note that there is no transverse emittance blow up in both beams, and the emittance growth is dominated by processes other than beam-beam interaction. The same is true for antiproton intensity and bunch length. The most pronounced difference between the observation and the model is seen in the proton intensity evolution. Beam-beam effects caused the proton lifetime degradation during the initial 2-3 hours of the store until the proton beam-beam tune shift drops from 0.02 to 0.015. The corresponding loss of the luminosity integral was about 5%.

4. Numerical simulations of beam-beam effects

Numerical simulations of beam-beam effects in the Tevatron were carried out with the use of weak-strong particle tracking code Lifetrac. Initially this code was developed for simulation of

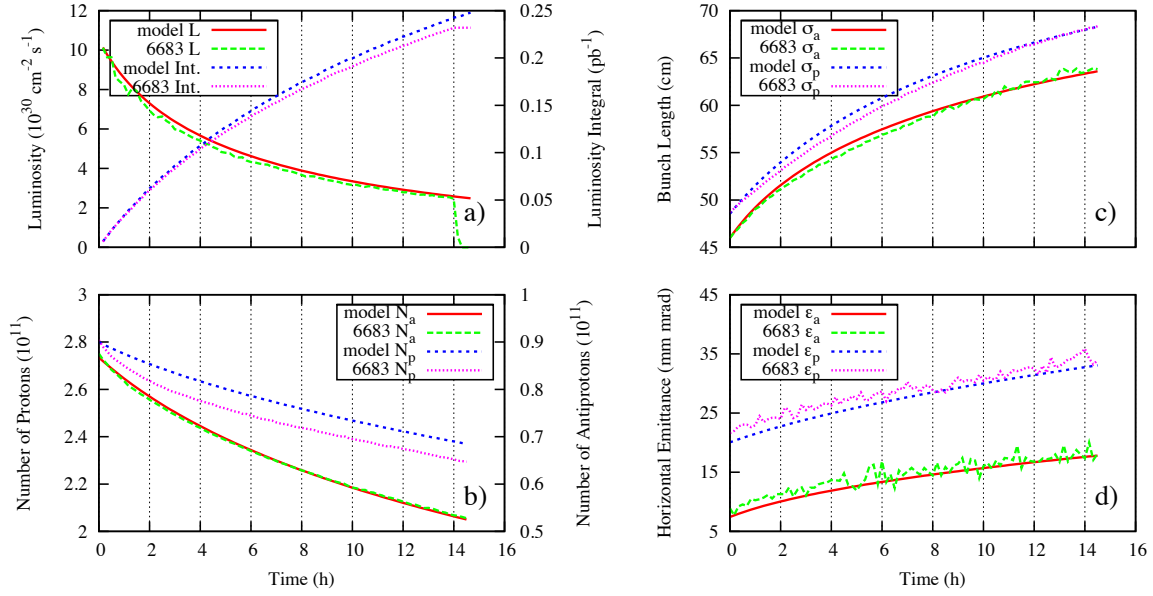


Figure 7. Observed beam parameters in store 6683 compared to store analysis calculation (model). $L_0 = 3.5 \cdot 10^{32} \text{cm}^{-2} \text{s}^{-1}$. a) single bunch luminosity and luminosity integral. b) intensity of proton bunch no. 6 and of antiproton bunch colliding with it (no. 13). c) rms bunch lengths. d) horizontal 95% normalized bunch emittances.

the equilibrium distributions of the particles in circular electron-positron colliders [16]. In 1999 the new features have been implemented, which allowed simulating non-equilibrium distributions, for example in proton beams. In this case the goal of simulations is not to obtain the equilibrium distribution but to observe the evolution of initial distribution. The number of simulated particles can vary in the range from 10^3 to 10^6 , usually it is set to $(5 \div 10) \cdot 10^3$. The tracking time is divided into “steps”, typically $10^3 \div 10^5$ turns each. The statistics obtained during the tracking (1D histograms, 2D density in the space of normalized betatron amplitudes, luminosity, beam sizes and emittances) is averaged over all particles and all turns for each step. Thus, a sequence of frames representing evolution of the initial distribution is obtained.

Another important quantity characterizing the beam dynamics is the intensity lifetime. It is calculated by placing an aperture restriction in the machine and counting particles reaching the limit. The initial and final coordinates of the lost particle are saved. This information is valuable for analysis of various beam dynamics features.

The initial 6D distribution of macroparticles can be either Gaussian (by default), or read from a separate text file. The macroparticles may also have different “weights”. This allows representing the beam tails more reliably with a limited number of particles. Usually we simulate the Gaussian distribution with weights: particles initially located in the core region have larger weights while the “tail” particles with smaller weights are more numerous.

In the Tevatron bunch pattern (3 trains of 12 bunches) there are two main IPs and 70 long range collision points for each bunch. When performing transformation through a main IP, the “strong” bunch is divided into slices longitudinally. The higher are the orders of significant betatron resonances which are supposed to make effect on the distribution, the greater must be the

number of slices. In our simulations 12 slices were used in the main IPs where beta-functions are approximately equal to the bunch length and only one slice in long range collision points where beta-functions are much greater and one can neglect the betatron phase advance over the bunch length.

The transverse density distributions within “strong” slices are bi-Gaussian, allowing to apply the well-known formulae [17] for the 6D symplectic beam-beam kick. However, a simple modification allowed simulating non-Gaussian strong bunches. Namely, the strong bunch is represented as a superposition of a few (up to three) Gaussian distributions with different betatron emittances. The kicks from all these “harmonics” are summarized additively. The calculation time is increased somehow (not very significantly) but the transformation remains 6D symplectic.

4.1 Tevatron optics

The parasitic collisions in Tevatron played significant role in the beam dynamics. In order to account for their contribution correctly, an accurate knowledge of the focusing optics of the whole ring with all distortions, beta beatings, coupling, etc. was required. This necessitated the construction of a realistic model of the machine lattice based on beam measurements. The most effective method proved to be the orbit response matrix analysis [18, 19, 20].

The model lattice was built in the optics code OptiM [21]. Both OptiM and Lifetrac treat betatron coupling using the same coupled beta-functions formalism [22]. That allows the linear transport matrix between any two points to be easily derived from the coupled lattice functions and phase advances.

A set of scripts has been created enabling fast creation of input files for the beam-beam simulation. These programs automate calculation of azimuthal positions of interaction points for the chosen bunch and extraction of the optics parameters. At the end, the machine optics is represented by a set of 6D linear maps between the interaction points.

It was estimated that resonances generated by known Tevatron nonlinearities, such as the final focus triplets and lattice sextupoles, were much weaker than those due to beam-beam collisions at the operational betatron tune working point. Hence, inclusion of nonlinear lattice elements into the simulation was deemed unnecessary. Still, the code has the capability to include thin multipoles up to the 10-th order.

4.2 Chromaticity

Although linear optics is used for the machine lattice model, there are two nonlinear lattice effects which are considered to be significant for beam-beam behaviour and were included into simulations. These are the chromaticities of beta-functions excited in the main IPs and chromaticities of the betatron tunes. In the Hamiltonian theory the chromaticity of beta-functions does not come from energy-dependent focusing strength of quadrupole magnets (as one would intuitively expect) but from drift spaces where the transverse momentum is large (low-beta regions). The symplectic transformations for that are:

$$\begin{aligned} X &= X - L \cdot X' \cdot \frac{\Delta p}{p} \\ Y &= Y - L \cdot Y' \cdot \frac{\Delta p}{p} \end{aligned}$$

$$Z = Z - L \cdot (X'^2 + Y'^2)/2$$

where X , Y , and Z are the particle coordinates, and L is the “chromatic drift” length. Then, it is necessary to adjust the betatron tune chromaticities which are also affected by “chromatic drift”. For that, an artificial element (insertion) is used with the following Hamiltonian:

$$H = I_x \cdot (2\pi Q_x + C_x \frac{\Delta p}{p}) + I_y \cdot (2\pi Q_y + C_y \frac{\Delta p}{p}),$$

where I_x and I_y are the action variables, Q_x and Q_y are the betatron tunes, C_x and C_y are the [additions to the] chromaticities of the betatron tunes.

4.3 Diffusion and noise

Diffusion and noise are simulated by a single random kick applied to the macroparticles once per turn. Strength of the kick at different coordinates is given by a symmetrical matrix representing correlations between Gaussian noises. In the Tevatron operation, the diffusion was rather slow in terms of the computer simulation – the characteristic time for the emittance change was about an hour, or $\sim 10^8$ turns. In our simulations of the beam-beam dynamics, the noise was artificially increased by three orders of magnitude in order to match the diffusion and the computer capabilities.

We justify this approach below. In contrast to electron-positron colliders there is no synchrotron radiation damping in hadron colliders. As the result, during the store time the effect of beam-beam interaction on the emittance growth needs to be minimized and made small relative to other diffusion mechanisms such as the intra-beam scattering (IBS), scattering on the residual gas, and diffusion due to RF phase noise, etc. We will call these the extrinsic diffusion to distinguish from the diffusion excited by beam-beam effects. For the 2005 Tevatron parameters the extrinsic diffusion set the luminosity lifetime to be about 10 hours at the beginning of the store. IBS dominated both transverse and longitudinal diffusions in the case of protons while its relative effect was significantly smaller for antiprotons because of ~ 5 times smaller intensity.

Table 1 summarizes lifetimes for major beam parameters obtained with diffusion model [23] for a typical 2005 Tevatron store with the luminosity of $0.9 \times 10^{32} \text{cm}^{-2} \text{s}^{-1}$. There were many parameters in Tevatron which are beyond our control and therefore each store was different. For good stores, the beam-beam effects made comparatively small contribution to the emittance growth yielding luminosity lifetime in the range of 7-8 hours and 10-15% loss in the luminosity integral.

Table 1. Lifetimes for major beam parameters obtained with diffusion model.

Parameter (lifetime, hour)	Protons	Antiprotons
Luminosity	9.6	9.6
Transverse emittance, ($d\varepsilon/dt$)/ ε [hor./vert.]	-17 / -18	-52 / -46
Longitudinal emittance	-8	-26
Intensity	26	155

Under the Tevatron operational conditions, the emittance growth rate was small and exact simulations of beam-beam effects would require tracking for billions of turns. That is well beyond

capabilities of present computers. Fortunately, the extrinsic diffusion is much faster than the beam diffusion. That leads to the loss of phase correlation after about 50,000 turns.

The external noise plays an important role in particle dynamics: it provides particle transport in the regions of the phase space which are free from resonance islands.

To make this transport faster we can artificially increase the noise level assuming that its effect scales as noise power multiplied by number of turns. If we choose it so that the noise alone gives 10% emittance growth in 10^6 turns (we use this level as the reference) then this number of turns of simulation will correspond to ~ 5 h of time in the Tevatron.

To verify this approach we studied the effect of the noise level on luminosity using the reconstructed optics.

Figure 8 presents the results of tune scan along the main diagonal with the reference noise level and without noise. The effect of noise on luminosity corresponds to its level with exception of the point $Q_y = 0.575$ where it was larger due to some cooperation with strong 5th order resonances.

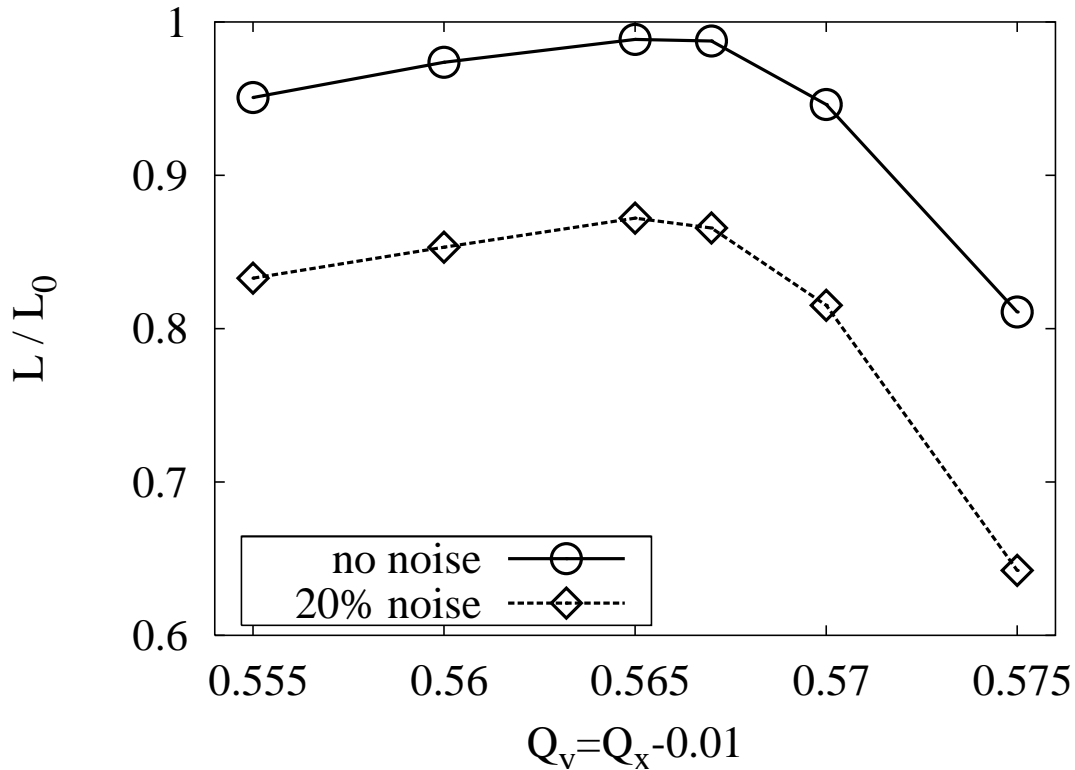


Figure 8. The reduction of luminosity after $t = 2 \cdot 10^6$ turns to the initial luminosity vs. betatron tune (simulations). Circles - no noise, diamonds - with noise amplitude corresponding to 20% emittance growth.

To study this cooperation in more detail we performed tracking at this working point with different noise levels. Fig.9 shows the luminosity reduction in $2 \cdot 10^6$ turns (diamonds) and a fit made using just 3 points, with relative noise level 0.5, 1 and 2.

The fit works fine for higher noise level, but predicts somewhat faster luminosity decay in the absence of noise than actually observed in tracking. This means that there are regions in the phase space which particles cannot pass (within the tracking time) without assistance from the external

noise so that the simple rule for diffusion coefficients D , $D_{total} = D_{beam-beam} + D_{noise}$ does not apply. However, such “blank spaces” may contain isolated resonance islands which would show up on a longer time scale with the real level of external noise. The applicability of this rule at the

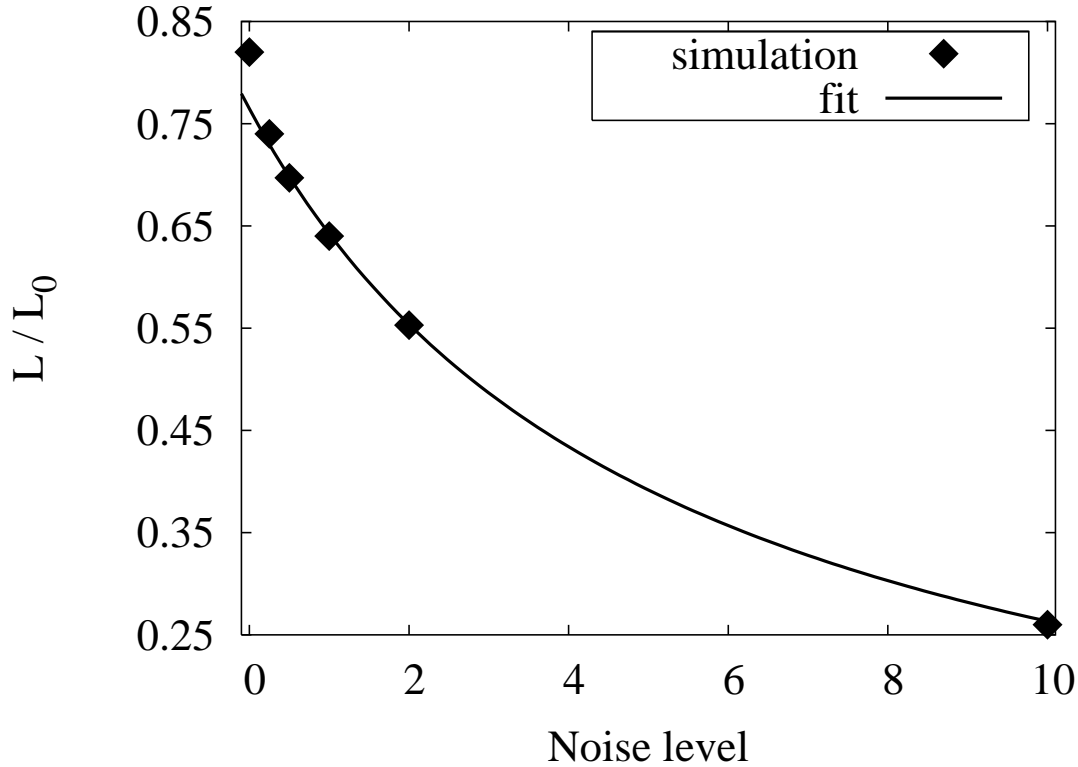


Figure 9. Reduction of luminosity after $2 \cdot 10^6$ turns vs. noise amplitude (simulations at $Q_y = 0.575$).

reference noise level testifies that (with the chosen number of turns) no such “blank spaces” were left so we get more reliable predictions.

Since 2007 we do no longer use the artificial noise enhancement for two reasons: a) the time interval of interest became shorter (less than one hour) after the shift of focus in beam-beam effects from antiprotons to protons; b) over the years the available computing power was constantly increasing and e.g. now, a full tracking over 10^7 turns (corresponding to 210 s of real time) takes about 20 hours on a modern computing cluster.

4.4 Program features

Since Lifetrac uses the “weak-strong” model, it can be very efficiently parallelized. Each processor tracks its own set of particles and the nodes need to communicate very rarely (at the end of each step), just to gather the obtained statistics. Hence, the productivity grows almost linearly with the number of nodes.

There are also two auxiliary GUI codes. The first one automates production of the Lifetrac input files for different bunches from the OptiM machine lattice files. The second one is dedicated

for browsing the Lifetrac output files and presenting the simulation results in a text and graphical (histogram) form.

4.5 Code validation

We have validated the code using available experimental data. As an example, Figures 10 and 11 show a good reproduction of the two distinct effects in the bunch to bunch differences caused by beam-beam effects: variation of vertical bunch centroid position due to long range dipole kicks, and variation of transverse emittance blowup caused by difference in tunes and chromaticities. We also demonstrated that scallops can be reduced by moving the working point farther from 5th order resonance.

In addition, Lifetrac was validated against another weak-strong tracking code Sixtrack on the case of the Large Hadron Collider, and good agreement was observed [24].

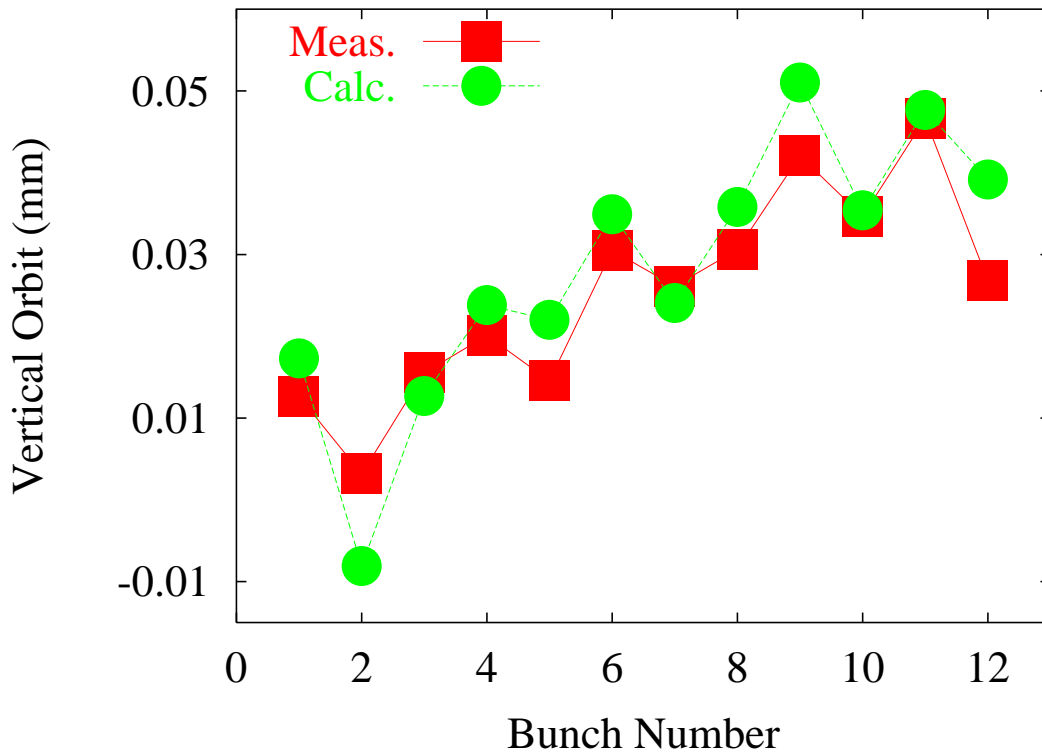


Figure 10. Bunch by bunch antiproton vertical orbit: squares - measurements, circles - Lifetrac simulations.

5. Simulation results

Simulations with Lifetrac played an important role in justification of many collider configuration changes, which resulted in performance improvements. These changes include the decrease of antiproton betatron tune chromaticity, reduction of the β^* from 0.35 m to 0.28 m (both in 2005), correction of the collision optics, increase of separation at the long range collision points nearest

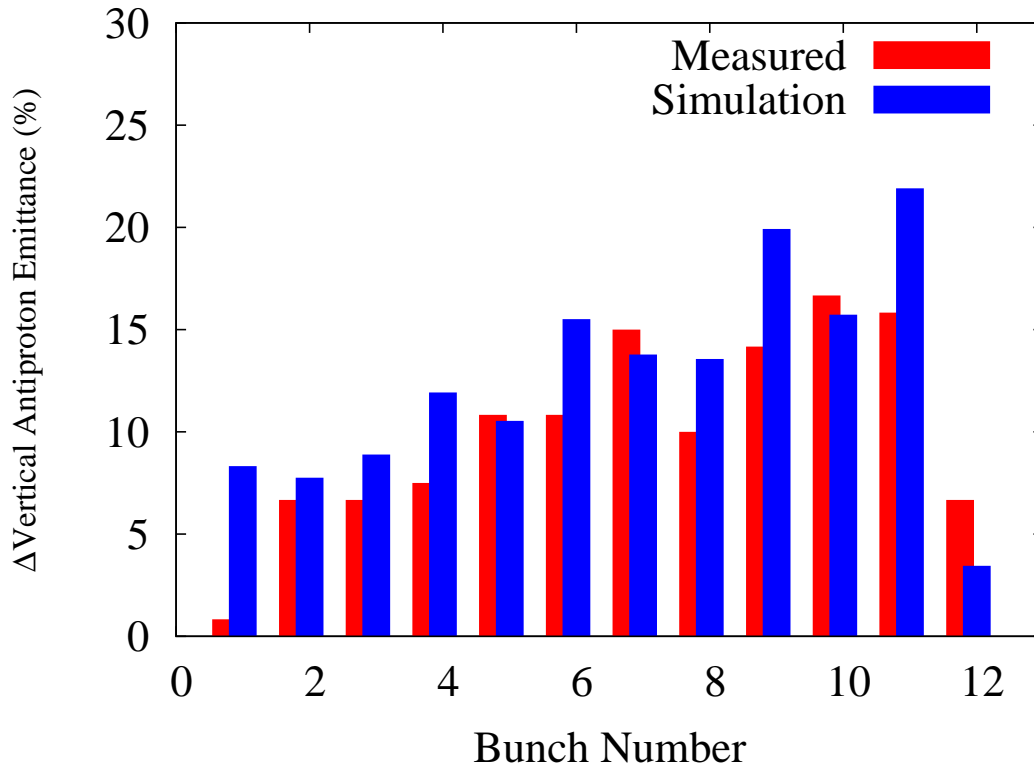


Figure 11. Bunch by bunch antiproton emittance growth. Measured in store 3554 (red) and simulated with Lifetrac (blue).

to the main IPs, and correction of the chromatic beta-function. In this section we present selected simulation results for some of these topics.

5.1 Optics errors

Early in the Collider Run II it was recognized that the Tevatron collision optics had significant deviations from design caused by the systematic betatron coupling resulting from the coil creep in main dipoles [25], magnet calibration errors and other sources. We have measured the machine optics using the orbit response method [18] and performed simulations with Lifetrac for different optics versions. In the results presented below we used 3 major optics modifications:

- “design” optics with ideal parameters of the main IPs and zero coupling.
- “january” optics which was in effect until March, 2004. This optics was measured in January, 2004, and had sufficient distortions in the main IPs (unequal β -functions, beam waists shifted from the IP), and betatron coupling.
- “june” optics introduced in March, 2004, where all the distortions were corrected.

Comparison of the three cases is shown in Figure 12. This plot shows that modifications to the optics implemented in March, 2004, made the optics close to the design. Additional simulations

revealed that the main source of particle losses was in the long range collisions nearest to the main IPs. Increasing the beams separation in those points and optimisation of the phase advances cured high antiproton losses.

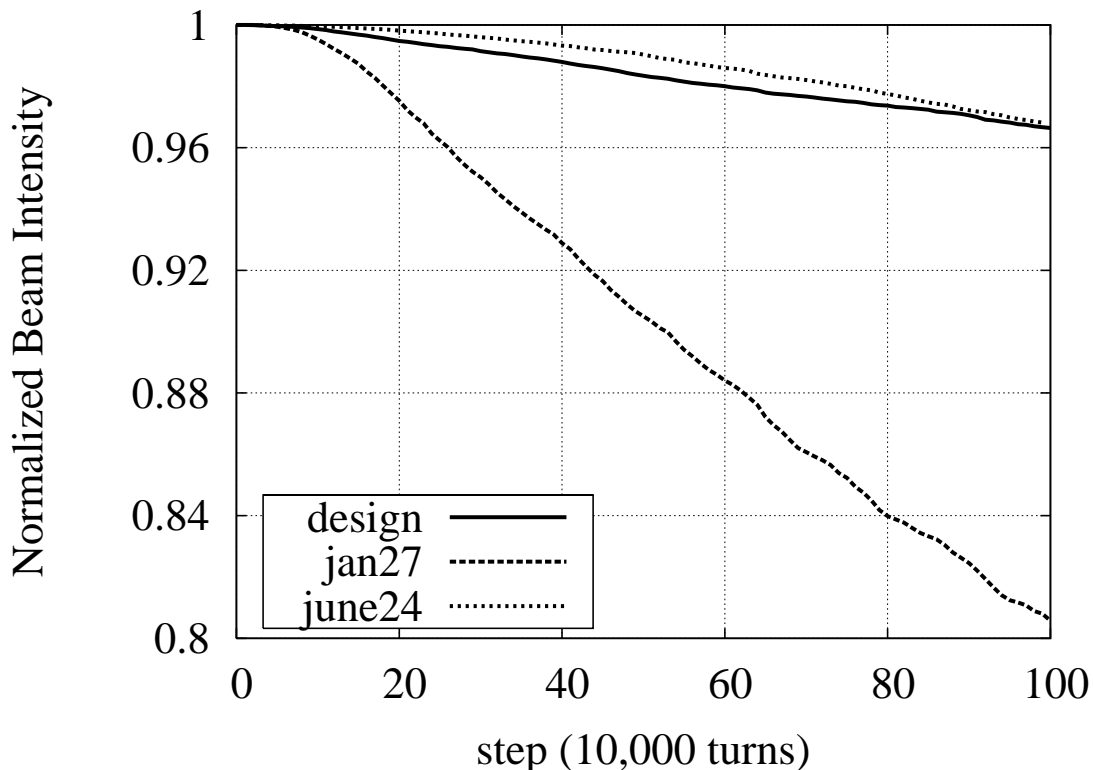


Figure 12. Intensity of antiproton bunch #6 vs. time for different types of optics (simulations with Lifetrac). $\xi = 0.01$, $Q_x = 0.57$, $Q_y = 0.56$

5.2 New collision helical separated orbit

As mentioned above, the strong betatron resonances affecting the collider performance were caused by beam-beam effects. It was shown analytically that the strength of the 7-th order resonance was determined by the long range collisions [8]. Our simulations predicted that increasing the beam separation at the parasitic collision (PC) points nearest to the main IPs would give the largest benefit. The significance of the PCs is illustrated in Figure 13, where a bunch intensity is plotted vs. time (2×10^6 turns in this simulation correspond to about 15 hours in the Tevatron) with the complete set of IPs and PCs, and with the most significant PCs turned off. It is clear that PCs dominate the particle losses.

To increase separation at these PCs, two extra electrostatic separators were installed during the 2006 shutdown. As the result, the separation at the PCs upstream and downstream of the main collision points (CDF and D0) increased by about 20% (Table 2). The larger separation showed itself in improved antiproton lifetime and allowed to push the proton intensity limit further.

Figure 14 shows a comparison of the single bunch luminosity and luminosity integral for two HEP stores before and after commissioning of the new helical orbits. Initial intensities and

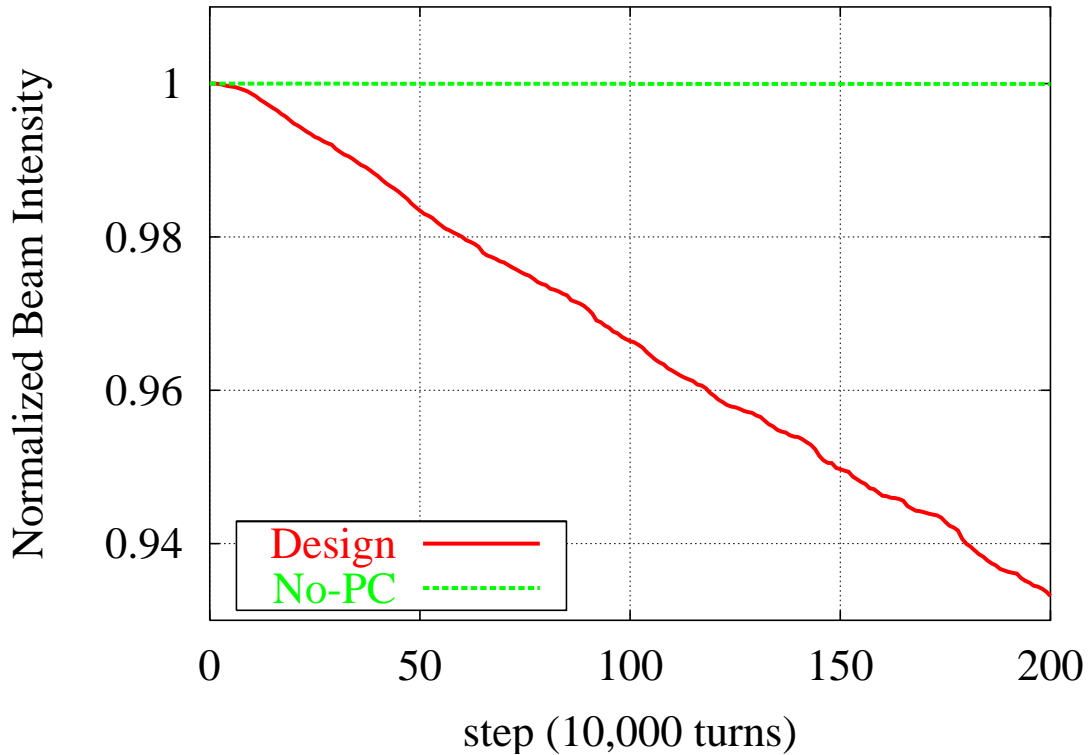


Figure 13. Normalized intensity of antiproton bunch #6 simulated in the presence (solid line) and in the absence (dashed line) of the parasitic beam-beam interactions.

Table 2. Radial separations in the first long range collision points in the units of the rms beam size.

	CDF u.s.	CDF d.s.	D0 u.s.	D0 d.s.
Before	5.4	5.6	5.0	5.2
After	6.4	5.8	6.2	5.6

emittances of antiprotons in these stores were close which allows direct comparison. As one can see, luminosity lifetime in the new configuration has substantially improved. The overall gain can be quantified in terms of luminosity integral over a fixed period of time (e.g. 24 hours) normalized by the initial luminosity. The value of this parameter has increased by 16%.

5.3 Betatron tune chromaticity

Reducing the betatron tune chromaticity can also be a very powerful instrument in decreasing the particle losses. Simulation results in Figure 15 demonstrate that changing the tune chromaticity from 15-20 units to 5-10 units may significantly improve the beam lifetime. This change was implemented in 2006 and resulted in about 10% gain in the luminosity integration rate. The safe lower limit of the tune chromaticity was determined by the coherent stability of the beams. It was demonstrated experimentally that with head-on collisions initiated, the beams remained stable even at zero chromaticity. Apparently, the Landau damping by strong nonlinearity of the head-on beam-

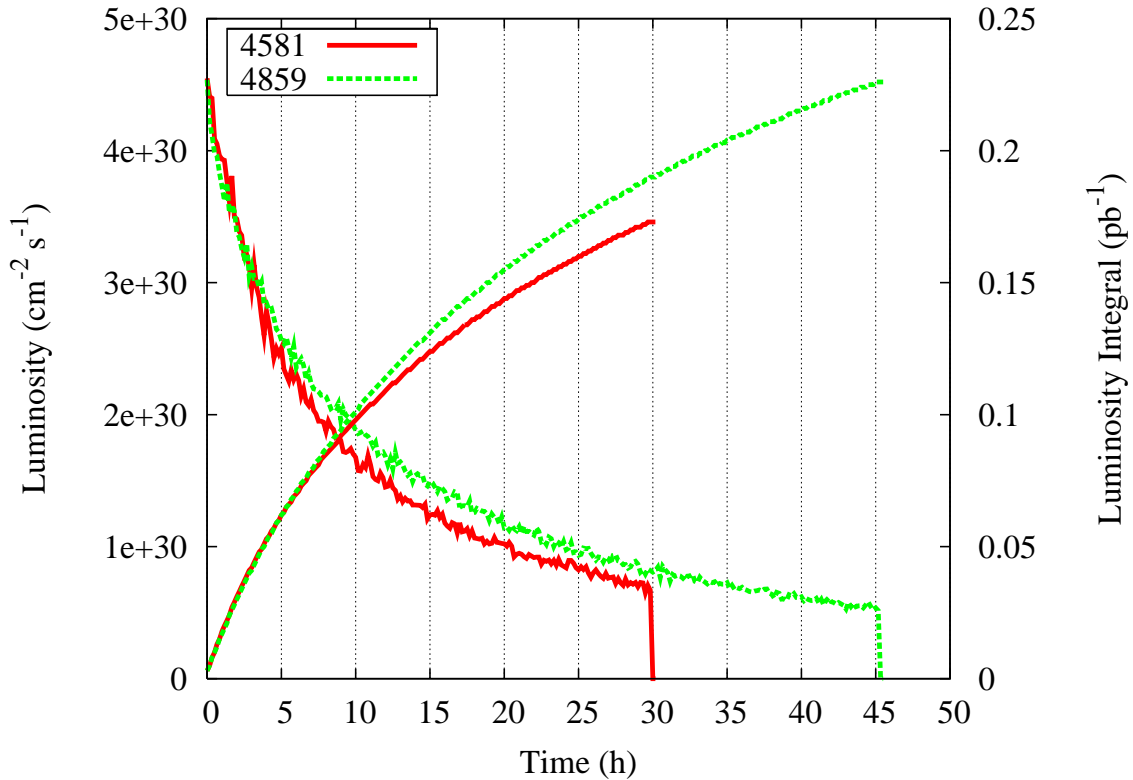


Figure 14. Single bunch luminosity and luminosity integral for stores 4581 and 4859 (correspondingly - before and after installation of additional electrostatic separators).

beam was the major factor. However, in the routine operation the typical value of chromaticity was set at approximately 5.

5.4 β^* reduction

Another improvement which could be relatively easily implemented was the reduction of the beta-function at the main IPs. Decreasing the β^* from the design value of 0.35 m to 0.28 m resulted in a 10% gain both in peak luminosity and in the luminosity integral. However, further improvement along this route was not practical due to the hourglass effect and rather significant increase of the maximum beta-function in the final focus triplet, and subsequent enhancement of effects related to the magnet vibrations and aperture limitation.

5.5 Second order chromaticity

Increasing the beam separation mitigated the long range beam-beam effects. However, with advances in the antiproton production rate, the initial antiproton intensity at collisions has been rising continuously. In 2006, the head-on beam-beam parameter for protons was pushed up to 0.016 which made the head-on beam-beam effects in the proton beam much more pronounced. One of the possible ways for improvement was a major change of the betatron tune in order to increase the available tune space (e.g. close to the half-integer). That, however, would require significant investment into the machine time for optics studies and tuning. A partial solution could be imple-

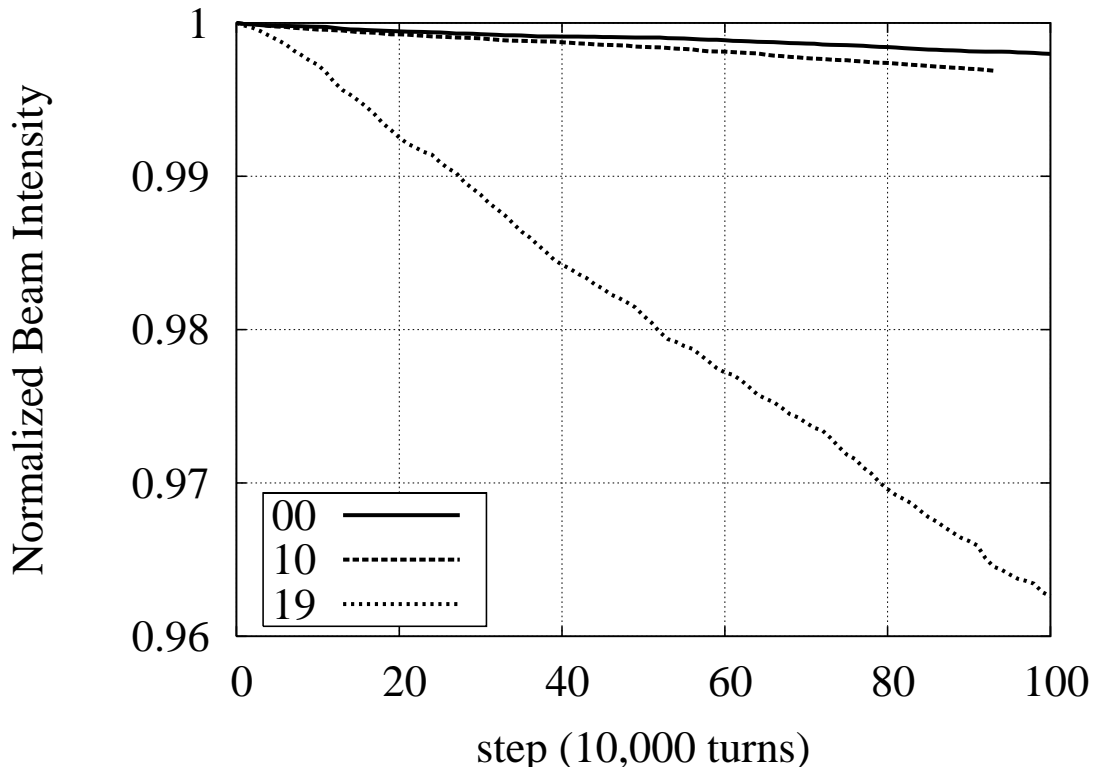


Figure 15. Evolution of the antiproton bunch intensity for various values of betatron tune chromaticity, $Q' = 0, 10, 19$. $Q_x = 0.58$, $Q_y = 0.575$, $\xi = 0.01$.

mented by decoupling of the transverse and longitudinal motion at the main IPs i.e., by reducing the chromatic beta-function.

The value of chromatic beta-function $(\Delta\beta/\beta)/(\Delta p/p)$ at both IPs in the original Tevatron lattice was -600 which lead to the beta-function change of 10% for a particle with 1σ momentum deviation [10]. Thus, a large variation of focusing for particles in the bunch existed giving rise to beam-beam driven synchrobetatron resonances.

Planning ahead for the increase in amount of antiprotons available to the collider, we identified the large chromaticity of β^* as a possible source of the proton lifetime deterioration. Figure 16 shows the beam-beam induced proton lifetime for different values of ξ , and demonstrates the beneficial effect of corrected chromatic β^* .

Simulations revealed an interesting feature in the behavior of the proton bunch length at high values of ξ – the so-called “bunch shaving”, when the bunch length starts to decrease after initiating head-on collisions instead of steady growth predicted by the diffusion model (Figure 17). This behavior was observed multiple times during HEP stores in 2007, being especially pronounced when the vertical proton betatron tune was set too high.

In order to achieve the desired smaller beta-function chromaticity, a new scheme of sextupole correctors in the Tevatron has been developed and implemented in May of 2007. The scheme used the existing sextupole magnets, which were split into multiple families instead of just two original SF and SD circuits. The effect of introducing the new circuits is illustrated in Figure 6.

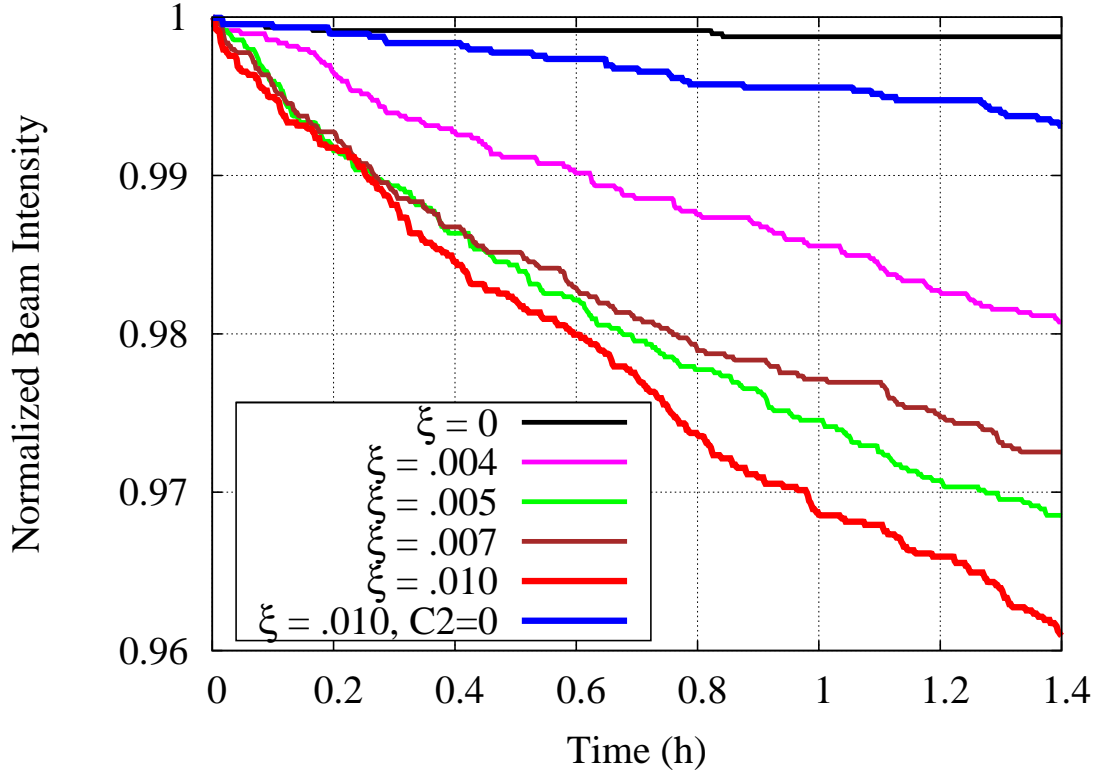


Figure 16. Proton intensity evolution for different values of the beam-beam tune shift parameter per IP from $\xi = 0$ to $\xi = 0.01$; without and with compensation of the chromaticity of β^* ($C_2 = 0$).

6. Summary and discussion

Over the last four years of the Collider Run II, Tevatron routinely operated at the values of head-on beam-beam tune shift for both proton and antiproton beams exceeding 0.02. The transverse emittance of antiprotons was a factor of 3 to 5 smaller than the proton emittance. This created significantly different conditions for the two beams.

Beam-beam effects in antiprotons were dominated by long range interactions at four parasitic collision points with minimal separation. After the separation at these points was increased to 6σ no adverse effects were observed in antiprotons at nominal proton intensities.

On the contrary, protons experienced intensity lifetime degradation due to head-on collisions with the beam of smaller transverse size. Correction of chromatic β -function in the final focus and reduction of betatron tune chromaticity increased the dynamic aperture and improved proton beam lifetime.

Weak-strong simulation of the beam-beam effects in the Tevatron with Lifetrac code correctly describes many observed features of the beam dynamics, has predictive power and has been used to initiate modifications of the machine configuration.

Further increase of the beam intensities was limited by the space available on the tune diagram near the operational working point. A change of the tune working point from 0.58 to near the half integer resonance would allow as much as 30% increase of intensities but would require a lengthy

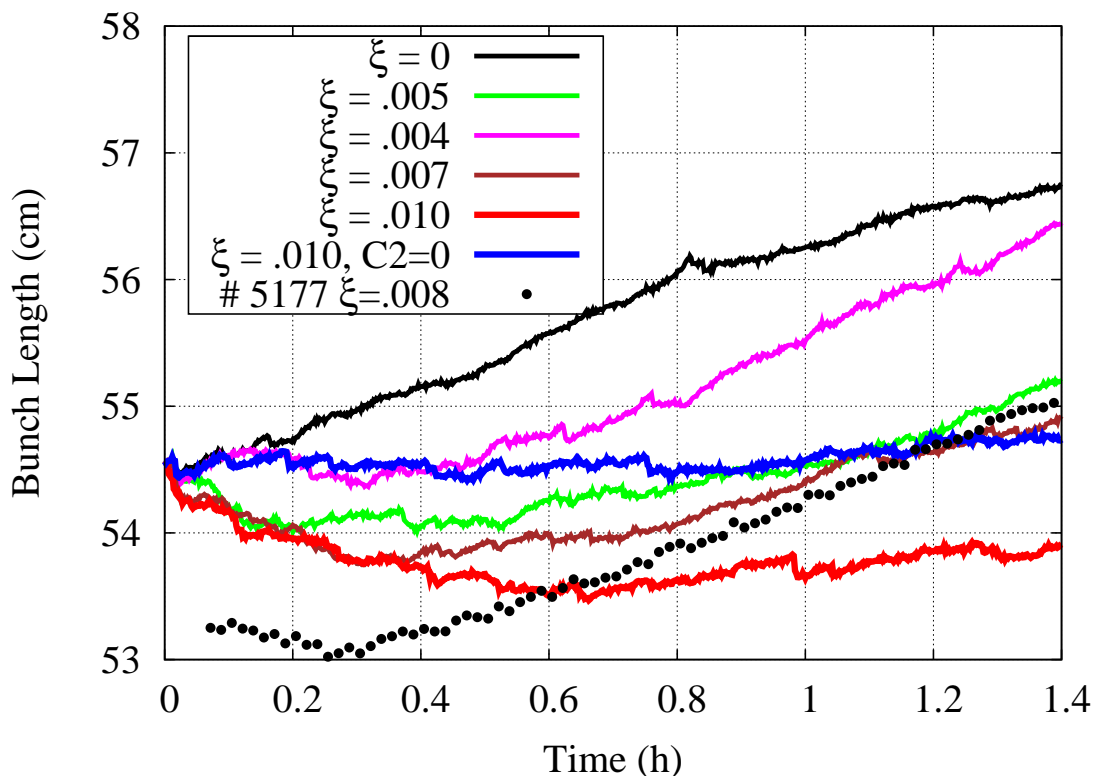


Figure 17. Effect of the corrected second order chromaticity ($C_2 = 0$) on the proton bunch length evolution at different values of the beam-beam parameter (solid lines - simulations, dots - Tevatron HEP store #5177).

commissioning period which rendered this improvement impossible in the Tevatron Collider Run II.

Acknowledgments

We would like to thank the Tevatron Department staff for their constant support and help in carrying out the beam experiments. We are particularly grateful to J. Annala, B. Hanna, R.S. Moore, V. Shiltsev, D. Still and C.Y. Tan. We would like to acknowledge the assistance of computing cluster administrator M. Kriss. We are indebted to T. Bolshakov for his help with the design of computer simulations. Fermilab is operated by Fermi Research Alliance, LLC under Contract No. DE-AC02-07CH11359 with the United States Department of Energy.

References

- [1] S. Holmes, R.S. Moore, and V. Shiltsev, *Overview of the Tevatron collider complex: goals, operations and performance*, 2011 *JINST* **6** T08001.
- [2] S. Nagaitsev et al., *Experimental demonstration of relativistic electron cooling*, *Phys. Rev. Lett.* **96** (2006) 044801.
- [3] V. Shiltsev et al., *Beam-beam effects in the Tevatron*, *Phys. Rev. ST Accel. Beams* **8** (2005) 101001.

- [4] P.M. Ivanov et al., *Head-tail instability at Tevatron*, in proceedings of *the 2003 IEEE Particle Accelerator Conference*, Portland, OR, USA, (2003), p. 3062.
- [5] P.M. Ivanov et al., *Landau damping of the weak head-tail instability at Tevatron*, in proceedings of *the 2005 IEEE Particle Accelerator Conference*, Knoxville, TN, USA, (2005), p. 2714.
- [6] V.H. Ranjbar and P.M. Ivanov, *Chromaticity and wakefield effect on the transverse motion of longitudinal bunch slices in the Fermilab Tevatron*, *Phys. Rev. ST Accel. Beams* **8** (2008) 084401.
- [7] R.S. Moore et al., *Improving the Tevatron collision helix*, in proceedings of *the 2005 IEEE Particle Accelerator Conference*, Knoxville, TN, USA, (2005), p. 1931.
- [8] Y. Alexahin, *Optimization of the helical orbits in the Tevatron*, in proceedings of *the 2007 IEEE Particle Accelerator Conference*, Albuquerque, NM, USA, (2007), p. 3874.
- [9] C.Y. Tan and J. Steimel, *Controlled emittance blow up in the Tevatron*, in proceedings of *the 2009 IEEE Particle Accelerator Conference*, Vancouver, BC, Canada, (2009), p. 1668.
- [10] A. Valishev et al., *Correction of second order chromaticity at Tevatron*, in proceedings of *the 2007 IEEE Particle Accelerator Conference*, Albuquerque, NM, USA, (2007), p. 3922.
- [11] V. Shiltsev and E. McCrory, *Characterizing luminosity evolution in the Tevatron*, in proceedings of *the 2005 IEEE Particle Accelerator Conference*, Knoxville, TN, USA, (2005), p. 2536.
- [12] M. Syphers, *Beam-beam tune distributions with differing beam sizes*, Fermilab internal report Beams Doc. 3031, (2008).
- [13] Yu. Alexahin, *Theory and reality of beam-beam effects at hadron colliders*, in proceedings of *the 2005 IEEE Particle Accelerator Conference*, Knoxville, TN, USA, (2005), p. 544.
- [14] V. Lebedev, *Beam physics at Tevatron complex*, in proceedings of *the 2003 IEEE Particle Accelerator Conference*, Portland, OR, USA, (2003), p. 29.
- [15] A. Valishev, *Tevatron store analysis package*, Software code supported in 2006-2011,
http://www-bd.fnal.gov/SDAViewersServlets/valishev_sa_catalog2.html
- [16] D. Shatilov, *Beam-beam simulations at large amplitudes and lifetime determination*, *Part. Accel.* **52** (1996) p. 65.
- [17] K. Hirata, H. Moshhammer and F. Ruggiero, KEK Report 92-117, (1992).
- [18] V. Sajaev et al., *Fully coupled analysis of orbit response matrices at the FNAL Tevatron*, in proceedings of *the 2005 IEEE Particle Accelerator Conference*, Knoxville, TN, USA, (2005), p. 3662.
- [19] A. Valishev et al., *Progress with collision optics of the Fermilab Tevatron collider*, in proceedings of *the 2006 European Particle Accelerator Conference*, Edinburgh, Scotland, (2006), p. 2053.
- [20] V. Lebedev et al., *Measurement and correction of linear optics and coupling at tevatron complex*, *Nucl. Instrum. Methods Phys. Res., Sect. A* **558**, (2006), p. 299.
- [21] V. Lebedev, *OptiM code*, Private communication,
<http://www-bdnew.fnal.gov/pbar/organizationalchart/lebedev/OptiM/optim.htm>
- [22] V. Lebedev and A. Bogacz, *Betatron motion with coupling of horizontal and vertical degrees of freedom*, 2010 *JINST* **5** P10010.

- [23] V. Lebedev and A. Burov, *Collective instabilities in the Tevatron complex*, in proceedings of the 33rd ICFA advanced beam dynamics workshop on high intensity and high brightness hadron beams, Bensheim, Germany, (2004), p. 350.
- [24] F. Schmidt, A. Valishev and Y. Luo, *Development and benchmarking of codes for simulation of beam-beam effects at the LHC*, BNL Note C-A/AP/443, (2011).
- [25] G.E. Annala, D.J. Harding and M.J Syphers, *Coil creep and skew-quadrupole field components in the Tevatron*, 2012 JINST 7 T03001.
- [26] V. Shiltsev and A. Tollestrup, *Emittance growth mechanisms in the Tevatron beams*, 2011 JINST 6 P08001.